EFFECT OF RHODIUM INFILTRATION ON THE MICROSTRUCTURE AND PERFORMANCE OF Ni/$Ce_{0.8}Gd_{0.2}O_{2-\delta}$ CERMET ANODE FOR LOW TEMPERATURE SOLID OXIDE FUEL CELL

F. S. Torknik[1*], M. Keyanpour-Rad[1], A. Maghsoudipour[1] and G. M. Choi[2]

* *fstorknik@gmail.com*

Received: Novamber 2015 **Accepted: January 2016**

[1] Materials and Energy Research Center, Tehran, Iran.

[2] Fuel Cell Research Center and Department of Materials Science and Engineering, Pohang University of Science and Technology, Pohang 790-784, Republic of Korea.

Abstract: *In order to further enhance the Ni/$Ce_{0.8}Gd_{0.2}O_{2-\delta}$ (Ni/GDC20) cermet anodic performance for low temperature solid oxide fuel cell (LT-SOFC), a study was conducted on the nanostructuring of NiO/GDC composite by only once wet-infiltration of rhodium chloride precursor. By using electrochemical impedance spectroscopy (EIS) analysis, the effect of only one drop of Rh-infiltrating solution on the anodic polarization resistance was examined using symmetric Ni–GDC20|GDC20|Pt electrolyte-supported cell at 400-600 °C. Nanostructural evolution before and after H_2 reduction at 600 °C and also after anodic performance test was investigated by atomic force microscopy (AFM), field emission scanning electron microscopy (FE-SEM), and transmission electron microscopy (TEM) techniques in comparison to the anode itself. Despite the fine distribution of Rh-infiltrated nanoparticles having average particle size of 11.7 nm, the results showed ineffectiveness and inability of the Rh-nanoparticles to succeed in decreasing of anodic polarization resistance for H_2 oxidation reaction in LT-SOFC.*

Keywords: *LT-SOFC, Anode, Ni/GDC cermet, Infiltration, Rhodium catalyst.*

[DOI: 10.22068/ijmse.13.1.43]

1. INTRODUCTION

Low temperature solid oxide fuel cells (LT-SOFCs) due to the improvement of their long-term durability, cost effectiveness [1, 2], and wider range of exploitable materials [3] have recently attracted much attention [1,2].But, to compensate the reduction in conversion efficiencies of fuels, the increase of inhibition by impurities (fuel flexibility) [4], and also the increase in ohmic and cell polarization losses at reduced temperatures [5], LT-SOFCs need to be developed for functional materials [6], i.e. catalysts and electrolytes with suitable catalytic and electrical properties, different from those commonly used for high temperature SOFC [3]. For this reason, ceria doped with rare-earth oxides, especially gadolinia-doped ceria (GDC) acts as a favorable component material used for fabrication of electrolytes and the anodes [7].

Nickel/GDC anodes have been successfully used as a cost-effective anodic material having high electrical conductivity for hydrogen or syngas fuels [8] in SOFCs [9]. However, due to limitation of the microstructure optimization associated with the high temperature sintering step of the anode preparation [10], some challenges like enhancement of the active reaction zone resulted from the contact zone between micro-sized particles have been remained [11]. Therefore, microstructural refinement of Ni/GDC porous anodes seems to be an appropriate approach to attain higher grain boundary density, extend the triple phase boundary (TPB) length that correlates with the reaction rate of H_2 oxidation [12].It also improves the surface exchange kinetic [9], decreases the electrode impedance [13], and improves the anodic performance [12]. This can be achieved through adjustment of powder morphology and particle size of NiO and GDC, and/or developing a favorable electrode processing [14]. For the initial efforts to engineer the anode microstructure, Torknik et al. have confirmed effectiveness of the high-energy milling method on disintegrating of the aggregates of NiO and $Ce_{0.8}Gd_{0.2}O_{2-\delta}$ (GDC20) to finer particle size powders. In addition, a finer-grained homogeneously distributed microstructure having lower anode polarization

resistance for the refined Ni/GDC anode has been also obtained [7]. For further extending of reaction sites and/or enhancing catalytic activity [15], addition of a slight amount of catalytically active agents or nanoparticles having hydrogen transport ability [16] via low temperature wet-infiltration/impregnation, can be an alternative, efficient, and cost-effective approach to nanostructuring [17]. Therefore, Torknik et al. have made subsequent attempt to deposit palladium nanoparticles on the refined Ni/GDC anode by PdCl2 loading. They have reported the significant decrease of anodic polarization resistance on highly Pd-infiltrated anode and less affinity of Pd-nanonetwork to coarsening (≤ 40 nm agglomerates) along with 45% oxidizing of Pd to PdO in H_2 environment [9].

Among the metal electrocatalysts having hydrogen transport ability [16], rhodium shows good activity. The effect of Rh wet impregnation in ceria-based anode shows that the performance is generally increased with addition of precious metal, however, the most significant improvement is observed with CH4 used as the fuel [18]. Study of H_2 production on the various substrates with 1wt% Rh catalyst at low temperatures (< 450 °C) shows higher activity of the Rh/ceria substrates, which also exhibit higher H2 yield at low temperatures, possibly due to efficient oxygen transfer from ceria to Rh [19]. The addition of 0.14 mg of Rh to the samaria-doped ceria (SDC) anode shows a significant effect on the performance of SDC (cathode)/YSZ/SDC (anode) cells [20]. Accordingly, nitrate precursor produces higher dispersion of rhodium phase [21] and also initial intrinsic activity and deactivation rate of Rh decrease with increasing metal particle size [22].However, based on the thermochemical data, it seems that Rh is a stable electrocatalyst at low operating temperatures [23].

In this paper, considering to the lower price of metal chloride than metal nitrates [24] and the importance of using least amount of cost-effective catalyst, nanostructuring of Ni/GDC anode by only addition of one drop of rhodium chloride precursor solution is carried out for comparing with a single infiltration of palladium chloride precursor. Microstructural refinement and anodic performance of Ni/GDC anodes are investigated using electron microscopy and electrochemical impedance spectroscopy, respectively.

2. EXPERIMENTAL PROCEDURE

Planar Ni–GDC20|GDC20 electrolyte-supported half-cells were used for the infiltration. Dense GDC20 electrolyte substrate with 15 mm diameter and ~0.3–0.4 mm thickness was prepared by tape casting, followed by sintering at 1400°C in the air for 5 h. NiO/GDC20 composite framework was prepared using a homogenized mixture of the modified $NiO_{0.6}$/$GDC20_{0.4}$ powder with the organic screen-printing solution and applied on the center of the electrolyte disc. The coated composite was sintered at 1350 °C in the air for 2 h to attain a porous microstructure having ~15 μm thickness and 0.5 cm^2 in area, as reported in detail in our previous work [9].

In order to make Rh- and Pd-infiltrated Ni/GDC20 anodes, the Rh- and Pd-containing solutions (0.1 mol/L) were prepared by dissolving $RhCl_3.3H_2O$ (H) and PdCl2 (D) (both MERCK) in deionized water and further dilution with hydrochloric acid, respectively. Infiltration was done using a micro syringe and placing a droplet of the metal chloride solution on NiO/GDC20 porous structure. Following the infiltration through capillary force, excess solution was wiped out from the surface of the anode, followed by calcination at 600 °C in the air for 1h.

Anodic impedance of the infiltrated Ni/GDC20 anodes was measured in the two-chamber conditions, using a three-electrode array [9]. Platinum paste was used in painting of the counter and reference electrodes, symmetrically opposite to the working electrode and a small point at the electrolyte edge, respectively and the mesh was used as a current-collector in intimate contact with the electrodes. Before testing, NiO in the anode composite was reduced insitu at 600 °C in H_2 environment for 1h. The electrochemical performance of the cermet anode was examined using an impedance analyzer (4192A, Hewlett-Packard) under open circuit potential with amplitude of 0.01 V in the frequency range 10

[DOI: 10.22068/ijmse.13.1.43]

Hz–1 MHz at the temperature range of 400–600 °C (50 °C steps). During the test, humidified hydrogen (97% H_2/3% H_2O) was used as the fuel gas with flow rate of 80 cc/min and open air as the oxidant. The anodic polarization resistance (Ra) as a measure of the anode's performance was obtained from the difference of the low and high frequency intercepts of the electrode arc on the real impedance axis of the Nyquist diagram. X-ray diffraction (XRD) was done for the composite using a D/Max-2500/PC Rigaku diffractometer with Cu Kα radiation (λ=1.540598 Å). Atomic force microscopy (AFM, VEECO Dimension 3100þNano scope V7) was used in tapping mode to image the topography and deflection of surface. Scanning electron microscopy (SEM, Philips XL30S FEG) was utilized in secondary electron (SE) mode to image the shape and size distribution of the infiltrated nanoparticles on the hydrogen-reduced cermets. The evaluations were performed in lacking of the coating materials before and after the cell testing (denoted with –R and –AT suffixes, respectively). Average particle size of the anode was determined using Digital Micrograph™ from 100 particles as minimum in an arbitrarily selected area. High-resolution transmission electron microscopy (HR-TEM, JEOL, JEM-2100F) was applied to study detailed microstructure of the anode with a point resolution of 0.1 nm in bright field (BF) mode. TEM specimen preparation was carried out by conventional method of suspension evaporating.

3. RESULTS AND DISCUSSION

3. 1. Microstructure of the Infiltrated Anodes

After the hydrogen reduction step, a poriferous fine-grained cermet with porous nickel particles, Ni and GDC grains of 30 nm and 207 nm, respectively, and porosity of 43% is obtained for the pure Ni/GDC (P-R) cermet (Fig.1a). As seen in Fig. 1b-c compared to Fig. 1a, the lack of particles with clean facets in the infiltrated cermets can be connected to a fully coverage of the composite surface in slight loading of ~ 0.03 mg/cm^2, however accumulation and aggregation of the infiltrated nanoparticles on the Ni particles is completely evident. Considering the easy observation of the Pd-infiltrated nanoparticles (D-R) by SEM, AFM inspection also confirms higher surface roughness, namely weaker wetting on the D-R (Fig. 2a) than H-R (Fig.2b). Furthermore, TEM evaluation of D-R (Fig. 3a) compared to H-R (Fig. 3b) indicates the average

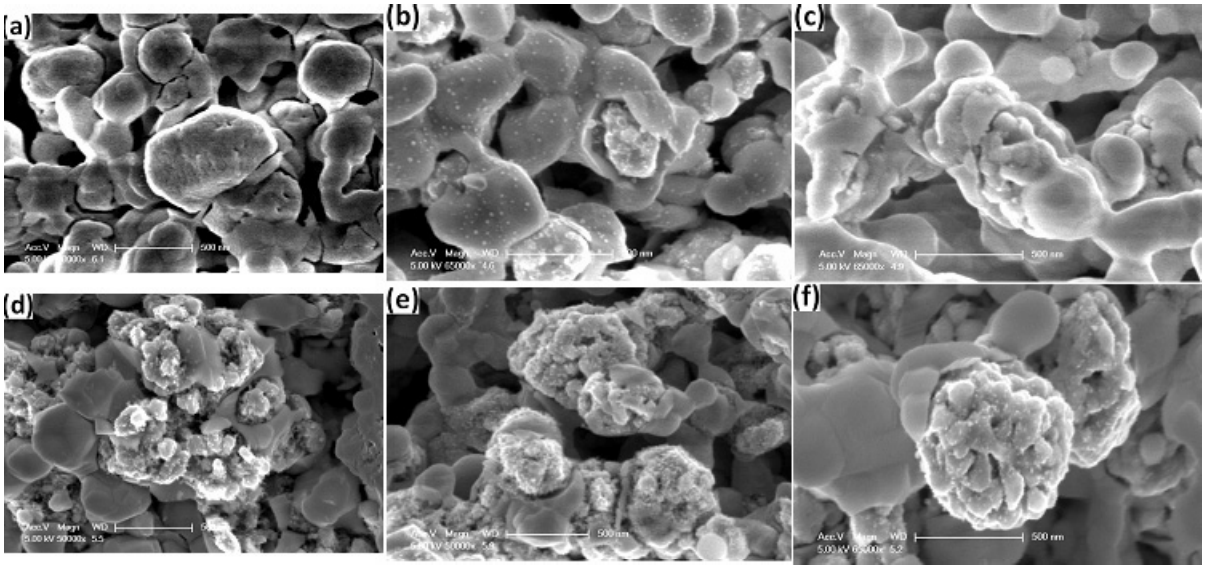

Fig. 1. SEM morphology of Ni/GDC cermets with/without infiltration of the nanoparticles before and after impedance test:(a)P-R,(b) D-R, (c) H-R, (d) P-AT, (e) D-AT, and (f) H-AT.

[DOI: 10.22068/ijmse.13.1.43]

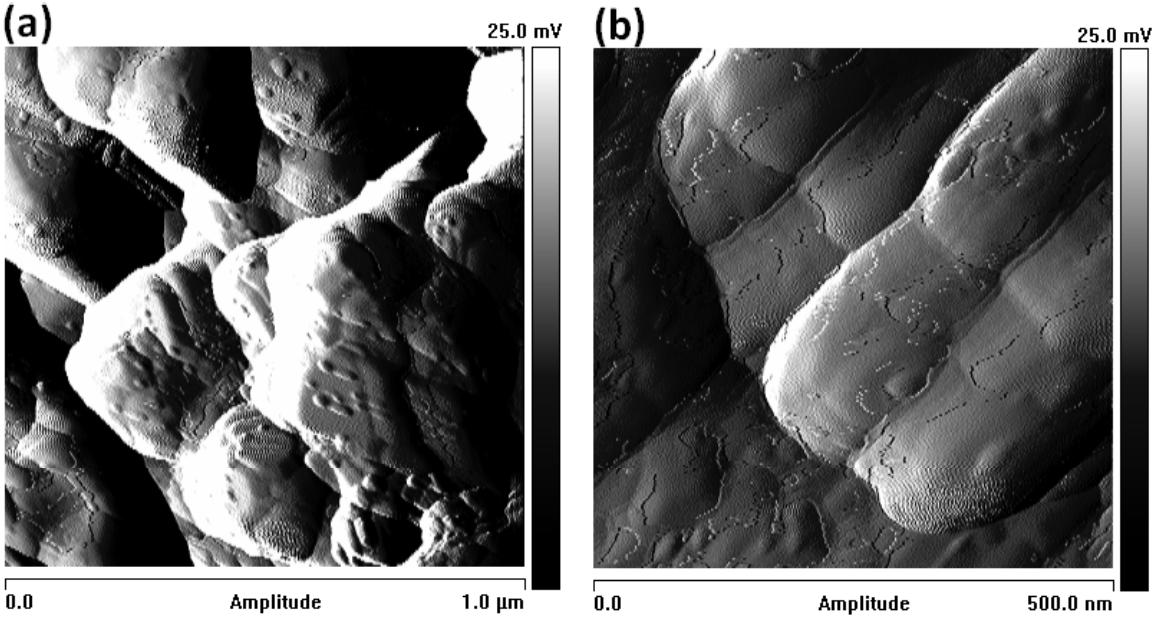

Fig. 2. AFM Amplitude image in two-dimension of (a) D-R and (b) H-R.

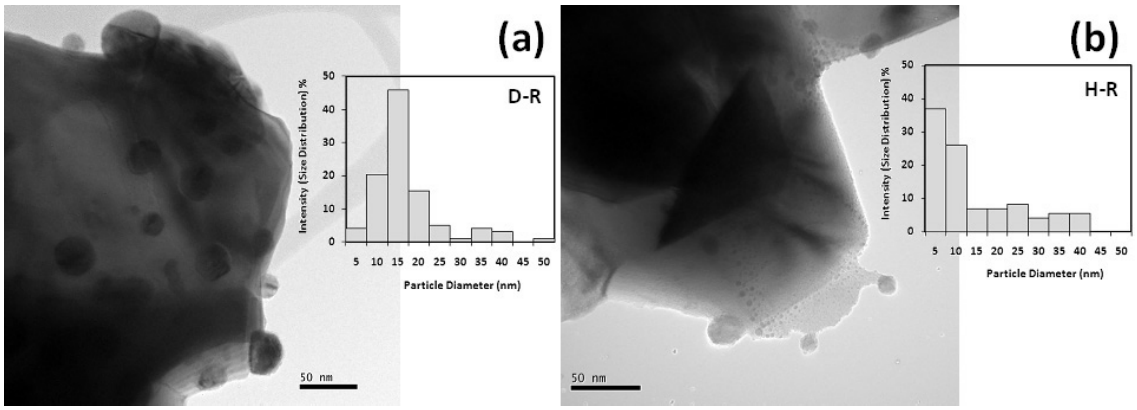

Fig. 3. Typical TEM-BF images and related nanoparticle size histograms obtained from the infiltrated cermet agglomerates of (a) D-R and (b) H-R.

nanoparticle size of ~ 14.4 nm and ~ 11.7 nm, respectively, matched to the SEM results, which confirms lower tendency of the Rh-nanoparticles for sintering at H2 than Pd-nanoparticles, as pointed out in the introduction. Electron diffraction investigation of the Pd-infiltrated cermet shows a minor amount of PdO left as unreduced species [9].

3. 2. Performance of the Infiltrated Anodes

Fig. 4 typically shows the impedance response of H_2 oxidation reaction on the infiltrated anodes, indicating lack of arc separation in the studied impedance frequency range. The Ra data for the infiltrated anode of D-Rat all the testing temperatures, as listed in table 1, show much lower amounts of Ra than that of H-R anode.

[DOI: 10.22068/ijmse.13.1.43]

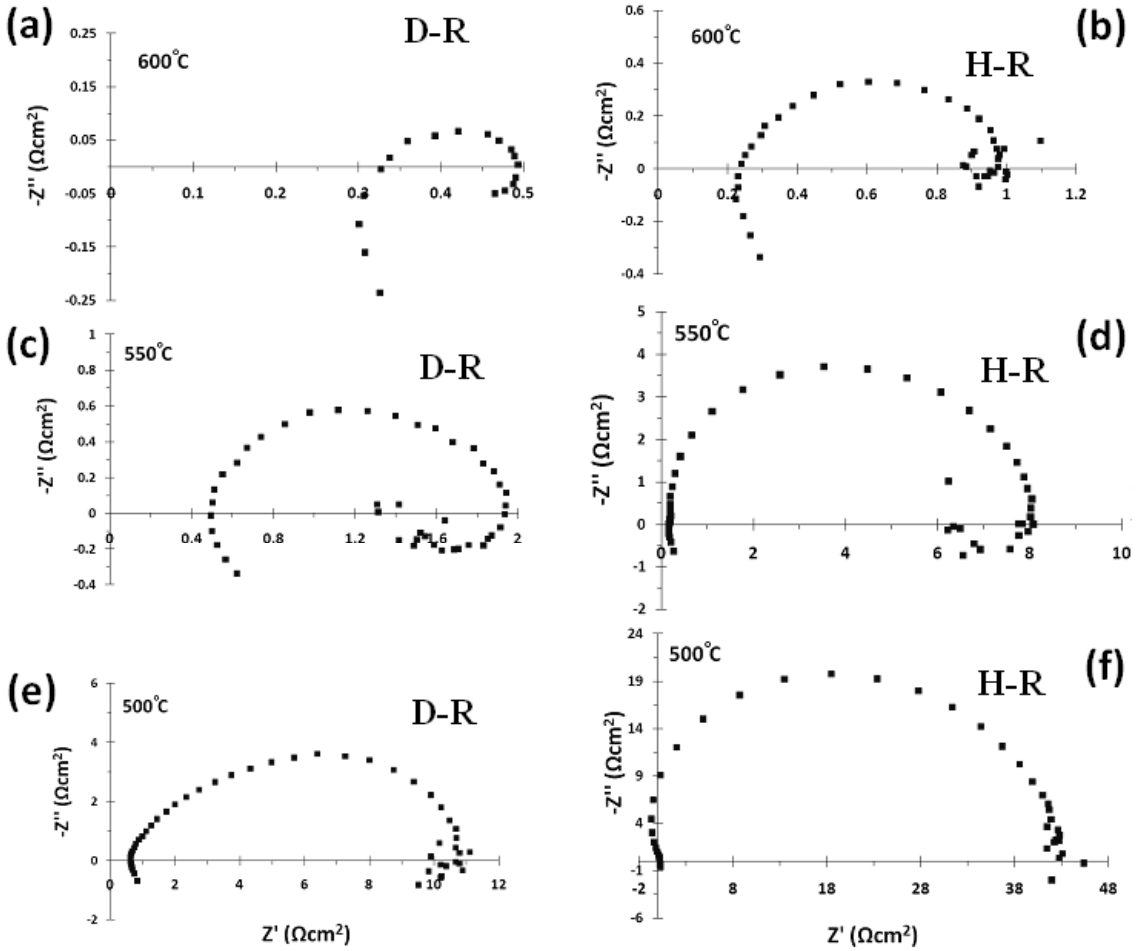

Fig. 4. Anodic impedance spectra for the H_2 oxidation reaction on the D-R and H-R anodes as a function of temperature in 97% H_2/3% H_2O at open circuit.

Table 1. Anode polarization resistance values for the H_2 oxidation reaction on the D-R and H-R anodes at testing temperatures in 97% H_2/3% H_2O at open circuit.

T (°C)	R_a (Ω.cm^2)				
	600	550	500	450	400
D-R	0.17	0.99	9.48	51.72	336.36
H-R	0.64	6.17	42.92	213.26	671.49

3. 3. Microstructure of the Infiltrated Anodes After Cell Testing

After anode testing in H_2 environment, the porosity of the P-AT cermet (Fig. 1d), due to the hydrogen accessibility to the Ni/NiO interfaceincreases1.5% (44.5%).SEM evaluation of D-AT (Fig. 1e) compared to H-AT (Fig. 1f) indicates that the average nanoparticle size of ~ 19 nm and ~ 16 nm, respectively. Less coarsening of H-AT can be related to the lower vaporization tendency of rhodium (10-30-10-20 Pa) than palladium (10-17-10-11 Pa)in H_2 environment at LT-SOFC, based on the partial pressure of catalytic metals [23] (Fig. 5). Although the decrease of intrinsic activity and deactivation rate of Rh with increasing metal particle size has been confirmed [22], but minor agglomeration of Rh-nanoparticles versus Pd-ones in similar conditions also cannot be a help for the effective electrocatalytic activity at LT-SOFC and hence Rh is a non-effective catalyst in our current study.

[DOI: 10.22068/ijmse.13.1.43]

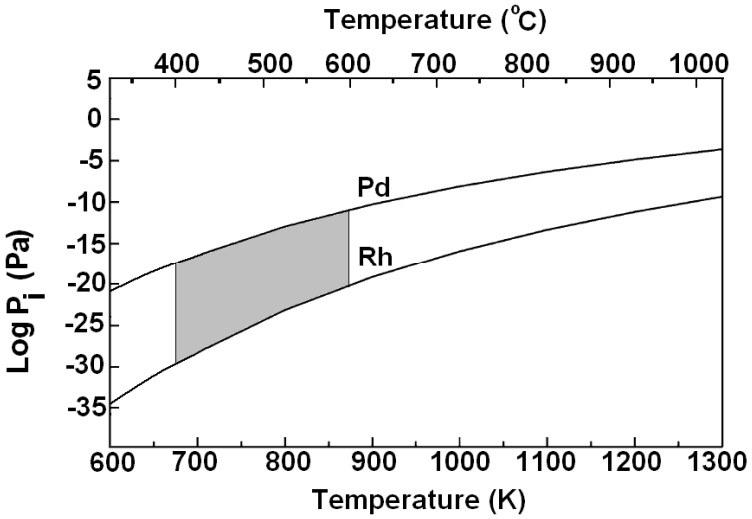

Fig. 5. Partial pressures of electro-catalytic metals [23].

Therefore, outstanding role of palladium for H_2 oxidation reaction can be attributed to the excellent catalytic properties and hydrogen absorption by palladium [25].

4. CONCLUSION

The investigation of nanostructure and anodic polarization resistance of Rh and Pd-infiltrated anodes with only addition of one drop of metal precursor solution for H_2 oxidation reaction at 400-600 °C shows that despite the less coarsening of fine Rh-nanoparticles at LT-SOFC, the anodic performance of Rh-infiltrated anode is much lower than Pd-infiltrated anode at all the temperatures. This indicates that using rhodium as an electrocatalyst for LT-SOFC is inefficient.

REFERENCES

1. Kilner, J. A., "Defects and Conductivity in Ceria-based Oxides". Chemistry Letters, 2008, 37, 1012-1015.
2. Steele, B. C. H., "Appraisal of $Ce_{1-y}Gd_yO_{2-y/2}$ electrolytes for IT-SOFC operation at 500°C". Solid State Ionics, 2000, 129, 95-110.
3. Modafferi, V., Panzera, G., Baglio, V., Frusteri, F. and Antonucci, P. L., "Propane reforming on Ni–Ru/GDC catalyst: H_2 production for IT-SOFCs under SR and ATR conditions". Applied Catalysis A: General, 2008, 334, 1–9.
4. Fergus, J. W., "Oxide anode materials for solid oxide fuel cells". Solid State Ionics, 2006, 177, 1529-1541.
5. Jiang, S. P. and Chan, S. H., "A review of anode materials development in solid oxide fuel cells". Journal of Materials Science, 2004, 39, 4405-4439.
6. Huang, J., Xie, F., Wang, C. and Mao, Z., "Development of solid oxide fuel cell materials for intermediate-to-low temperature operation". International Journal of Hydrogen Energy. 2012, 37, 877–883.
7. Torknik, F. S., Keyanpour-Rad, M., Maghsoudipour, A. and Choi, G. M., "Effect of microstructure refinement on performance of $Ni/Ce_{0.8}Gd_{0.2}O_{1.9}$ anodes for low temperature solid oxide fuel cell". Ceramics International, 2014, 40, 1341–1350.
8. Xu, C., Gansor, P., Zondlo, J. W., Sabolsky, K. and Sabolsky, E. M., "An H_2S-Tolerant Ni-GDC Anode with a GDC Barrier Layer". Journal of The Electrochemical Society, 2011, 158, 1405-1416.
9. Torknik, F. S., Maghsoudipour, A., Keyanpour-Rad, M., Choi, G. M., Oh, S. H. and Shin, G.-Y., "Microstructural refinement of $Ni/Ce_{0.8}Gd_{0.2}O_{2-\delta}$ anodes for low-temperature

[DOI: 10.22068/ijmse.13.1.43]

solid oxide fuel cell by wet infiltration loading of PdCl2". Ceramics International, 2014, 40, 12299–12312.

10. Babaei, A., Jiang, S. P. and Li, J., "Electrocatalytic Promotion of Palladium Nanoparticles on Hydrogen Oxidation on Ni/GDC Anodes of SOFCs via Spillover". Journal of the Electrochemical Society, 2009,156, 1022-1029.
11. Uchida, H., Suzuki, H. and Watanabe, M., "High-performance electrode for medium temperature solid oxide fuel cells: effects of composition and microstructures on performance of ceria-based anodes". Journal of The Electrochemical Society, 1998,145, 615–620.
12. Boer, B. de, Gonzalez, M., Bouwmeester, H. J. M. and Verweij, H., "The effect of the presence of fine YSZ particles on the performance of porous nickel electrodes". Solid State Ionics, 2000,127, 269–276.
13. Lee, W., Jung, H. J., Lee, M. H., Kim, Y.-B., Park, J. S., Sinclair, R. and Prinz, F. B., "Oxygen surface exchange at grain boundaries of oxide ion conductors". Advanced Functional Materials, 2011, 22, 965–971.
14. Zha, S., Rauch, W., Liu, M., "Ni-$Ce_{0.9}Gd_{0.1}O_{1.95}$ anode for GDC electrolyte-based low-temperature SOFCs". Solid State Ionics, 2004,166, 241–250.
15. Liu, Z., Ding, D., Liu, B., Guo, W., Wang, W. and Xia, C., "Effect of impregnation phases on the performance of Ni-based anodes for low temperature solid oxide fuel cells". Journal of Power Sources, 2011,196, 8561–8567.
16. Gade, S. K., Keeling, M. K., Davidson, A. P., Hatlevik, O. and Way, J. D., "Palladium–ruthenium membranes for hydrogen separation fabricated by electroless co-deposition". International Journal of Hydrogen Energy, 2009, 34, 6484–6491.
17. Jiang, S. P., "Nanoscale and nano- structured electrodes of solid oxide fuel cells by infiltration: Advances and challenges". International Journal of Hydrogen Energy, 2012, 37, 449-470.
18. McIntosh, S., Vohs, J. M. and Gorte, R. J., "Effect of Precious-Metal Dopants on SOFC Anodes for Direct Utilization of Hydrocarbons". Electrochemical and Solid-State Letters, 2003, 6, 240-243.
19. Roh, H. -S., Wang, Y. and King, D. L., "Selective Production of H_2 from Bio-Ethanol at Low Temperatures over Rh/CeO_2-ZrO_2 Catalyst". Topics in Catalysis, 2008, 49, 32–37.
20. Putna, E. S., Stubenrauch, J., Vohs, J. M. and Gorte, R. J., "Ceria-Based Anodes for the Direct Oxidation of Methane in Solid Oxide Fuel Cell". Langmuir, 1995, 11, 4832-4837.
21. Nowosielska, M., Jozwiak, W. K. and Rynkowski, J., "Physicochemical Characterization of Al_2O_3 Supported Ni–Rh Systems and their Catalytic Performance in CH_4/CO_2 Reforming". Catalysis Letters, 2009, 128, 83–93.
22. Irusta, S., Cornaglia, L. M. and Lombardo, E. A., "Hydrogen Production Using Ni—Rh on ZrO_2 as Potential Low-Temperature Catalysts for Membrane Reactors". Journal of Catalysis, 2002, 210, 263–272.
23. Barin, I. and Platzki, G., "Thermochemical data of pure substances", 3rd ed., VCH Verlagsgesellschaft mbH, Weinheim, 1995, DOI: 10.1002/9783527619825.
24. Arteaga, G. J., Anderson, J. A. and Rochester, C. H., "Effects of Catalyst Regeneration with and without Chlorine on Heptane Reforming Reactions over Pt/Al_2O_3 and $Pt–Sn/Al_2O_3$". Journal of Catalysis, 1999, 187, 219-229.
25. Adams, B. D. and Chen, A., "The role of palladium in a hydrogen economy". Materials today, 2011, 14, 282-289.

[DOI: 10.22068/ijmse.13.1.43]